Robotica (2019) volume 37, pp. 1090–1103. © Cambridge University Press 2019
doi:10.1017/S0263574718001479

Simultaneous Gravity and Gripping Force Compensation Mechanism for Lightweight Hand-Arm Robot with Low-Reduction Reducer

Mitsunori Uemura†*, Yuki Mitabe‡ and Sadao Kawamura‡

†*School of Engineering Science, Osaka University, Osaka, Japan*
‡*Department of Robotics, Ritsumeikan University, Shiga, Japan*

(Accepted December 20, 2018. First published online: January 14, 2019)

SUMMARY
In this paper, we propose a novel mechanism to compensate for gravity and the gripping force in a hand-arm robot. This mechanism compensates for the gravitational torque produced by an object gripped by the hand-arm robot. The gripping force required for the robot hand to prevent the object from dropping is also simultaneously compensated for. This mechanism requires only one actuator placed on the shoulder part of the robot. Therefore, this mechanism can reduce the torque requirement of joint actuators and lower the weight of the robot. The gear ratio of the reduction gears in each robot joint can then also be reduced. These advantages are critical for future robots that perform tasks in unstructured environments and collaborate with humans. We carried out experiments with a 6-DoF robot arm having a 1-DoF gripper to demonstrate the effectiveness of the proposed mechanism.

KEYWORDS: Gravity compensation; Gripping force compensation; Hand-arm robot; Wire-driven robot; Lightweight robot; Low-reduction reducer.

1. Introduction

Robots operating in unstructured environments unintentionally contact objects frequently. Robots collaborating with humans have to ensure safety when contacting humans. Although future robots will have to carry out these operations, most current robots may damage the objects or themselves when contacting the objects. A cause of this problem is that current hand-arm robots have high body weight and motor reducers with high reduction ratios in order to produce strong forces on the end effectors.

This problem can be overcome by imparting mechanical softness to the robots.[1–7] Mechanical softness absorbs impulsive forces and enables robots to carry out contact tasks. Much research has recently been conducted on imparting mechanical softness to robot arms,[2,3] actuators,[4,5] and transmission mechanisms.[6,7] However, mechanical softness produces higher order dynamics and can degrade control performance. Therefore, mechanical softness may not be the ideal solution when robots have to carry out precise or dexterous tasks.

The other way to overcome the problem is to reduce the weight of the robots and the gear ratio of the motor reducers. Asada and Youcef-Toumi proposed direct-drive and semi-direct-drive robots that utilize motor reducers with a low gear ratio.[8,9] These direct-drive and semi-direct-drive robots do not suffer from degraded control performance. However, direct-drive and semi-direct-drive actuators

* Corresponding author. E-mail: uemura-m@me.es.osaka-u.ac.jp

produce less torque than actuators with the same weight and high-reduction reducers. Reducing the torque requirement of robot joints then becomes a key issue. Wire-driven robots are effective for reducing the torque requirement of robot joints.[10–16] Wire-driven robots especially reduce the weight of the arm part, which is the most movable part of robot arms, by removing actuators from it. The inertia and gravity effect of the robot arm are then greatly reduced, and this leads to a reduced torque requirement. Gravity compensation mechanisms can further reduce the torque requirement of robot joints.[17–23] These mechanisms utilize passive mechanical elements, such as springs and counterweights, to compensate for the gravity torque produced not only by robots[17–20,22,23] but also by objects held by the robots.[21] The robots do not then consume any power while maintaining postures statically, and the gravity compensation mechanisms reduce the weight of the robot arms and the reduction ratios of the motor reducers.

However, the previous wire-driven robot arms and gravity compensation mechanisms have not considered weight reduction of robot hands. Although some wire-driven robot hands have been designed,[24–26] they are independent of the arm design. Robot hands are placed at the tip of hand-arm robots, where inertia or gravity forces mostly affect the torques of robot joints. Therefore, reducing the weight of robot hands is crucial to reduce the weight of robot arms and the reduction ratio of motor reducers.

This paper proposes a novel mechanism that simultaneously compensates for the gravity torque produced by a gripped object and the gripping force required for a robot hand to grip the object. This mechanism is driven by only one actuator mounted on the shoulder part of the hand-arm robot. Therefore, the proposed mechanism greatly reduces the torque requirement of joint actuators not only in the arm part but also in the hand part. This reduces the robot weight, especially the weight of the hand-arm part, and the reduction ratio of the motor reducers. This mechanism utilizes the characteristic that the force compensating for the weight of the gripped object and the force required to grip the object are proportional in principle. From the viewpoint of biomechanics, the proposed mechanism seems to be reasonable and interesting because the major muscle that produces human grip forces, the superficial flexor muscle, also produces the flexion torques of the wrist and elbow joint that are required to compensate for the gravity of the gripped object.

In this paper, we also propose a new structure for the wire-driven robot equipped with the proposed compensation mechanism. In the proposed wire-driven mechanism, an actuator mounted on the shoulder part of the robot drives the robot hand, although actuators mounted on the arm or hand part drive robot hands in previous wire-driven robots.

We developed wire-driven robots with the proposed mechanism, and experimental results with the developed robot demonstrate the effectiveness of the proposed mechanism.

2. Simultaneous Gravity and Gripping Force Compensation Mechanism

In this section, we propose a simultaneous gravity and gripping force compensation mechanism. The proposed mechanism is based on the self-weight compensation mechanism proposed by Hirose *et al*.[18]

2.1. Self-weight compensation mechanism[18]

Hirose *et al.* proposed a self-weight compensation mechanism for a 6-DoF robot arm.[18] This mechanism utilizes parallel linkages and a wire as shown in Fig. 1. A great advantage of this mechanism is that only one counterweight placed on the base part compensates for the gravity torques produced by the robot arm in all joints statically. Therefore, the torque requirement of the joint actuators can be reduced, which in turn reduces the weight of the robot arm and reduction ratios of the motor reducers.

Here, we describe the compensation principle of this mechanism. The parallel linkage of this mechanism keeps the sub-links vertical structurally. The compensation links are rigidly fixed to the main links. Taking into consideration the moment arm, the wire tension $T \in \mathbb{R}$ then produces the following compensation torque $\tau_{ci} \in \mathbb{R}$ at the $i \in \mathbb{N}$th joint:

$$\tau_{ci} = T l_{ci} \sin q_i, \tag{1}$$

where $l_{ci} \in \mathbb{R}$ is the compensation link length from the ith joint to the wire pulley, and $q_i \in \mathbb{R}$ is the joint angle between the ith sub-link and main link. By considering the parallel linkage again, the potential energy of each link, $p_i \in \mathbb{R}$, from the reference posture $q_i = \frac{\pi}{2}$ $(i = 1, 2, 3)$ is described as

https://doi.org/10.1017/S0263574718001479 Published online by Cambridge University Press

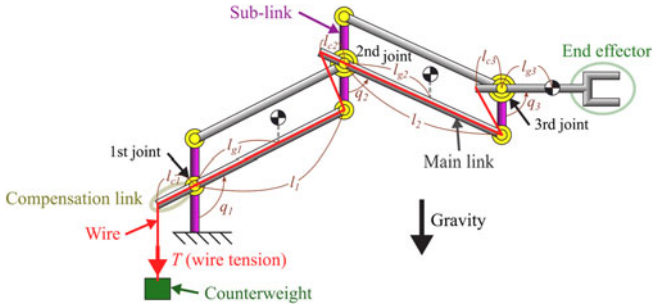

Fig. 1. Self-weight compensation mechanism.

$$p_i = m_i g \left(l_{gi} \cos q_i + \sum_{j=1}^{i-1} l_j \cos q_j \right), \tag{2}$$

where m_i is the total mass of the ith links, $g \in \mathbb{R}$ is the acceleration of gravity, $l_{gi} \in \mathbb{R}$ is the length from the ith joint to the mass center of the ith links, and $l_i \in \mathbb{R}$ is the link length of the ith main link. The robot arm then produces the following gravity torque at the ith joint:

$$\tau_{gi} = -\left(m_i g l_{gi} + \sum_{j=i+1}^{3} m_j g l_i \right) \sin q_i . \tag{3}$$

Equations (10) and (6) have a similar form. In addition, these parameters l_{ci}, m_i, g, l_i, and l_{gi} are constants, and the wire tension T is also statically the same constant as the gravity force of the counterweight. By setting these parameters to

$$T l_{ci} = m_i g l_{gi} + \sum_{j=i+1}^{3} m_j g l_i , \tag{4}$$

the weight of the robot is exactly compensated for $\tau_{gi} + \tau_{ci} = 0$ regardless of the joint angles q_i.

2.2. Gravity and gripping force compensation

The self-weight compensation mechanism greatly reduces the torque requirement of the robot actuators. However, the previous gravity mechanisms[17–23] have not considered compensation for the gripping force that is required when the robot grips an object. A large actuator torque is required to prevent an object from dropping, and consequently, the robot hand becomes heavier. Therefore, a hand-arm robot can normally pickup an object having a weight that is much lower than the weight capacity of the robot arm. Moreover, a robot hand is positioned at the tip of the robot, and the inertia and the weight of the hand greatly affect the torque requirement of joint actuators. Therefore, reducing the weight of the robot hand crucially lowers both the weight of the robot and the reduction ratios of the motor reducers.

2.2.1. Compensation mechanism. This paper proposes a mechanism that simultaneously compensates for gravity and the gripping force as shown in Fig. 2. This mechanism adopts parallel linkage, which is almost the same as the self-weight compensation mechanism. This mechanism also employs the wire to compensate for the gravity torques. A difference from the self-weight compensation mechanism is that the wire is fixed on the gripper to compensate for the gripping force. Another difference is that the proposed mechanism utilizes an actuator instead of a counterweight to handle objects with various weights. In this mechanism, only one actuator placed on the base part compensates for the gravity and gripping force simultaneously. Therefore, the proposed mechanism greatly reduces the torque requirement of the other joint actuators even when the robot grips objects with various weights. By adding a yaw axis at the base part and yaw and roll axes at the wrist part, we can develop a 6-DoF robot arm with a hand based on this mechanism.

https://doi.org/10.1017/S0263574718001479 Published online by Cambridge University Press

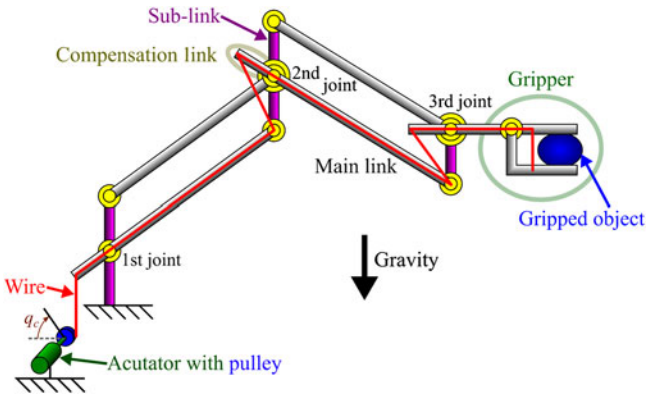

Fig. 2. Schematic of simultaneous gravity and gripping force compensation mechanism.

2.2.2. Principle of gravity compensation. The principle of the proposed mechanism is described as follows. The potential energy of a gripped object $p \in \mathbb{R}$ is given by

$$p = mg \sum_{i=1}^{3} l_i \cos q_i, \tag{5}$$

where $m \in \mathbb{R}$ denotes the mass of the gripped object. The gravity force of a gripped object then produces the following torque at the ith joint:

$$\tau_{gi} = -mgl_i \sin q_i. \tag{6}$$

The wire tension T produces the same compensation torque at the ith joint as Eq. (10). Therefore, the gravity force is exactly compensated for by setting the length of the compensation links l_{ci} and the wire tension T to $Tl_{ci} = mgl_i$ regardless of the joint angles. Because these parameters l_{ci}, m, g, and l_i are constants, the constant wire tension T, which is proportional to the mass of the object m, can compensate for the gravity force. When the weight of the gripped object m is changed, the compensation actuator adjusts the wire tension T for the gravity compensation.

2.2.3. Principle of gripping force compensation. Next, we describe the gripping force compensation of the proposed mechanism. When the robot hand grips an object with the weight m under the conditions shown in Fig. 3(a) and (b), the following gripping force $f \in \mathbb{R}$ is necessary to prevent the object from dropping:

$$f = \frac{mgs}{\mu}, \tag{7}$$

where $\mu \in \mathbb{R}$ is the coefficient of static friction satisfying $0 < \mu < 1$, and $s \in \mathbb{R}$ is the safety factor, which is greater than 1. Under the condition shown in Fig. 3(c), the following force f_g is necessary to compensate for the gravity of the gripped object:

$$f_g = mg. \tag{8}$$

The above shows that a force proportional to the mass of the gripped object is necessary to compensate for the force required for gripping the object, as in the case of gravity compensation. Therefore, by attaching a wire to the gripper as shown in Fig. 2, the gravity and the grasping force can be compensated for simultaneously.

2.2.4. Wire tension adjustment. We can consider some ways to adjust the wire tension.

One technique is to use the force of a compensation actuator with a motor reducer directly as shown in Fig. 2. An advantage of this method is mechanical simplicity. In this case, the dynamics of the compensation actuator is expressed by

https://doi.org/10.1017/S0263574718001479 Published online by Cambridge University Press

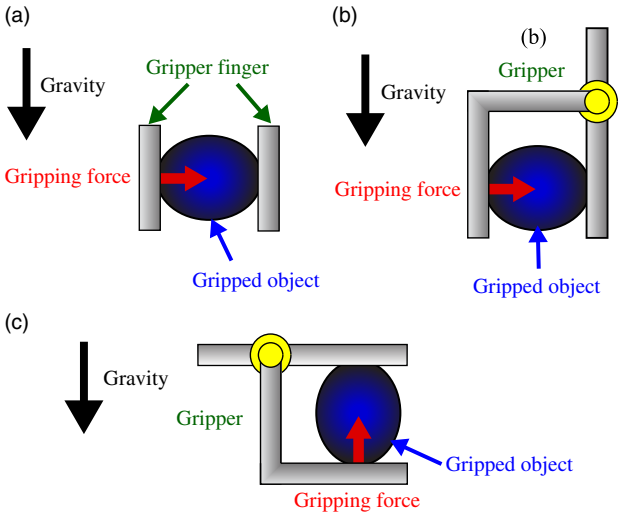

Fig. 3. (a)–(c) Gripping force necessary for gripping an object.

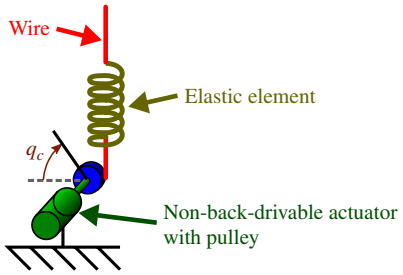

Fig. 4. Wire tension adjustment via series elastic actuator.

$$I_c\ddot{q}_c = a\tau_c - Tr_c - \tau_{fric}, \tag{9}$$

where $I_c \in \mathbb{R}$ is the inertia moment of the compensation actuator with the motor reducer and the pulley, $q_c \in \mathbb{R}$ is the angle of the pulley, $a \in \mathbb{R}$ is the reduction ratio of the motor reducer, $\tau_c \in \mathbb{R}$ is the torque exerted by the compensation actuator, $r_c \in \mathbb{R}$ is the radius of the pulley, and $\tau_{fric} \in \mathbb{R}$ is the friction torque of the compensation actuator with the motor reducer. The simplest controller that adjusts the wire tension T to the desired one $T_d \in \mathbb{R}$ is described as

$$\tau_c = \frac{T_d r_c}{a}. \tag{10}$$

Statically, the wire tension T is then adjusted to

$$T = T_d - \tau_{fric}. \tag{11}$$

If we ignore the friction torque τ_{fric}, the wire tension T is adjusted to the desired one T_d. However, the proposed compensation mechanism requires a large wire tension in typical cases, and this leads to large friction τ_{fric} and inertial $I_c\ddot{q}_c$ torques. These torques are transmitted to the robot joints through the wire tension. Therefore, a disadvantage of this wire tension adjustment method is that the dynamics of the compensation actuator with a motor reducer, such as friction and inertia, affects the robot joints. Another disadvantage is that continuous power consumption is required for the compensation actuator to maintain the compensation torque as seen in Eq. (10).

Another method of adjusting the wire tension is to use a series elastic actuator,[6] namely, to transmit the force of the compensation actuator via an elastic element as shown in Fig. 4.

In this case, the dynamics of the compensation actuator is expressed by

$$I_c\ddot{q}_c = a\tau_c - \tau_{fric} - k(r_c q_c - l_w)r_c \tag{12}$$

$$T = k(r_c q_c - l_w), \tag{13}$$

https://doi.org/10.1017/S0263574718001479 Published online by Cambridge University Press

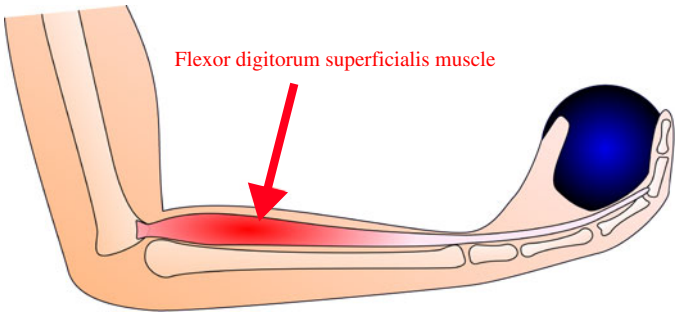

Fig. 5. Flexor digitorum superficialis muscle.

where $k \in \mathbb{R}$ is the stiffness of the elastic element, and $l_w \in \mathbb{R}$ is the length of the path along the wire and the elastic element from the point where the wire is fixed to the gripper pulley to the point where the wire contacts the pulley of the compensation actuator. Equation (13) means that the friction torque τ_{fric} and the inertial torque $I_c\ddot{q}_c$ do not directly affect the wire tension T. This is an advantage of this wire tension adjustment method. We can design the following PID controller to adjust the wire tension T to the desired one T_d.

$$\tau_c = \frac{k_{ci}\int_0^t (q_d - q_c)\mathrm{d}t + k_{cp}(q_d - q_c) - k_{cv}\dot{q}_c}{a} \tag{14}$$

$$q_d = \frac{T_d}{kr_c}, \tag{15}$$

where k_{ci}, k_{cp}, and $k_{cv} \in \mathbb{R}$ are the coefficients for the integral, proportional, and derivative terms, respectively. After the pulley angle q_c converges to the desired one q_d, the wire tension T becomes

$$T = T_d - kl_w. \tag{16}$$

Therefore, by selecting the stiffness of the elastic element k to low one, the wire tension T is adjusted to the desired one T_d. In this case, the friction torque τ_{fric} can even be effectively utilized. By adopting a non-back drivable mechanism as the motor reducer, the friction torque τ_{fric} maintains constant pulley angle q_c without using electrical power. Therefore, another advantage of this wire tension adjustment method is that power consumption is not required when the robot retains its grip on a certain object. A disadvantage of this method is mechanical complexity.

All these methods have their advantages and disadvantages, and we can select the method that is appropriate to the situation.

2.2.5. Self-weight compensation. The proposed mechanism does not consider self-weight compensation directly. Nevertheless, the proposed mechanism can compensate the self-weight of the robot with a certain degree of accuracy for the following reason. The self-weight of the robot can be equivalently converted to the hand mass with a certain degree of accuracy. The proposed mechanism can then compensate for the gravity torque produced by the converted hand mass and thus compensate for the self-weight of the robot with a certain degree of accuracy.

2.2.6. Analogy with human arm. In order to discuss the proposed mechanism from the viewpoint of biomechanics, we here consider the flexor digitorum superficialis muscle, which is one of the main muscles that produce the gripping force of human hands.

The flexor digitorum superficialis muscle is attached to the bones of the four fingers and the upper arm as shown in Fig. 5. The muscle thus contributes not only to the gripping force but also to the flexion torque of the wrist and elbow. The force and torque are required simultaneously when lifting a heavy object. In other words, the flexor digitorum superficialis muscle efficiently produces the torques of multiple joints required in a typical situation by a single muscle.

https://doi.org/10.1017/S0263574718001479 Published online by Cambridge University Press

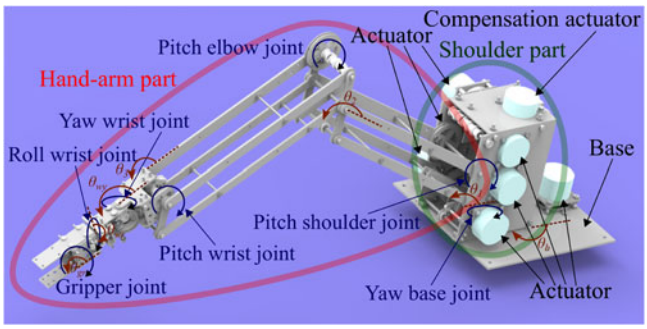

Fig. 6. Structure of wire-driven hand-arm robot with simultaneous gravity and grasping force compensation mechanism.

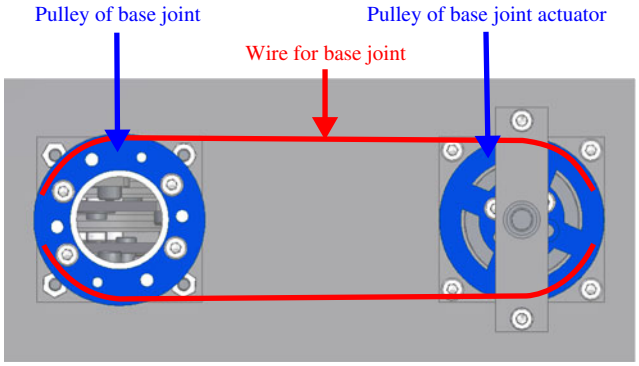

Fig. 7. Wire path for base joint (bottom view of base).

In addition, the centroid of the flexor digitorum superficialis muscle is located far away from the human hand. This is possibly to reduce the mass of the tip part as much as possible.

These characteristics are the same as those of the mechanism proposed in this paper. The proposed mechanism is hence reasonable and interesting also from the viewpoint of biomechanics.

3. Developed Wire-driven Hand-Arm Robot

We designed a wire-driven hand-arm robot with the gravity and gripping force compensation mechanism as shown in Fig. 6. In this robot, all actuators are not positioned on the hand or the arm part. Therefore, the hand-arm part, which is the main movable part of the robot, can be greatly reduced in weight. To the best of our knowledge, there is no existing wire-driven robot in which an actuator placed in the shoulder part produces a hand force. Therefore, this wire-driven mechanism is a novel one, which lowers both the weight of the robot and the reduction ratio of the motor reducers.

3.1. Structure

The proposed structure has seven rotational joints: a yaw joint at the base part; three pitch joints at the shoulder, elbow, and wrist parts; yaw and roll joints at the wrist part; and a pitch joint at the gripper. Seven DC motors with pulleys actuate these seven joints. Each joint has a pulley to receive the actuation force from each DC motor through wires. Enough tension is always applied to all the wires to prevent slack.

A DC motor fixed on the base actuates the yaw base joint. The pulleys of the DC motor and the yaw base joint are directly connected by the two wires to transmit bidirectional torque as shown in Fig. 7. The other six DC motors are fixed on the shoulder part. One of the DC motors actuates the shoulder joint using such a direct wire connection as shown in Fig. 8. The pulleys fixed to another DC motor and the elbow link are connected by two wires via a joint idling pulley as shown in Fig. 8. Each of the two wires is wound around the joint idling pulley once. The rotational axis of the joint idling pulley is identical to that of the shoulder joint. The wire paths then become independent of the

https://doi.org/10.1017/S0263574718001479 Published online by Cambridge University Press

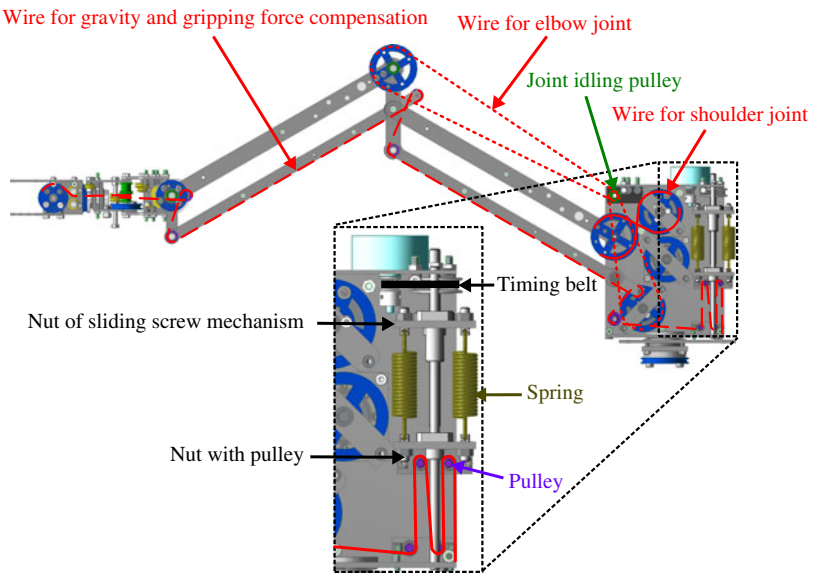

Fig. 8. Wire path for shoulder joint, elbow joint, and gravity and gripping force compensation (side view: some parts are made transparent to show the internal structure).

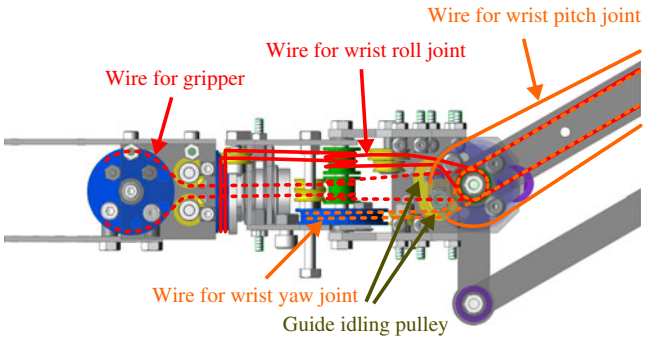

Fig. 9. Wire path for wrist pitch, yaw, and roll joint and gripper (side view).

joint angles. The diameter of the joint idling pulley is much smaller than that of the joint and actuator pulleys. The DC motor can then produce a torque for the elbow joint almost independently. The other joint idling pulleys play the same role.

The pulleys of another DC motor and the pitch wrist joint are connected by the two wires via the joint idling pulleys of the shoulder and elbow as shown in Fig. 9. Each of the remaining pulleys attached at the wrist roll joint and the gripper joint is connected to a pulley of a DC motor by two wires also via these joint idling pulleys. The wires for the wrist yaw joint pass through the guide idling pulleys as shown in Fig. 9. The guide idling pulleys guide the paths of the wires to make the paths independent of the joint angles. The other guide idling pulleys play the same role. Each of the pulleys for the yaw wrist joint and the gripper is also connected to a pulley of a DC motor by two wires via the joint and guide idling pulleys as shown in Fig. 9.

We adopted the method in which the wire tension for the gravity and gripping force compensation is produced by a series elastic actuator. An additional DC motor is fixed on the shoulder part for the gravity and gripping force compensation. This DC motor rotates the screw of the sliding screw mechanisms as shown in Fig. 8. One side of the springs is fixed to the nut of the sliding screw mechanism. The other side of springs is fixed to the other nut, which has pulleys. The wire is fixed to the gripper pulley and the shoulder part via the idling pulleys and the nut pulleys. The DC motor can then adjust the wire tension by expanding or contracting the spring. The compensation actuator did not consume any electric power when maintaining a certain compensation force because the sliding screw mechanism was substantially non-back drivable.

https://doi.org/10.1017/S0263574718001479 Published online by Cambridge University Press

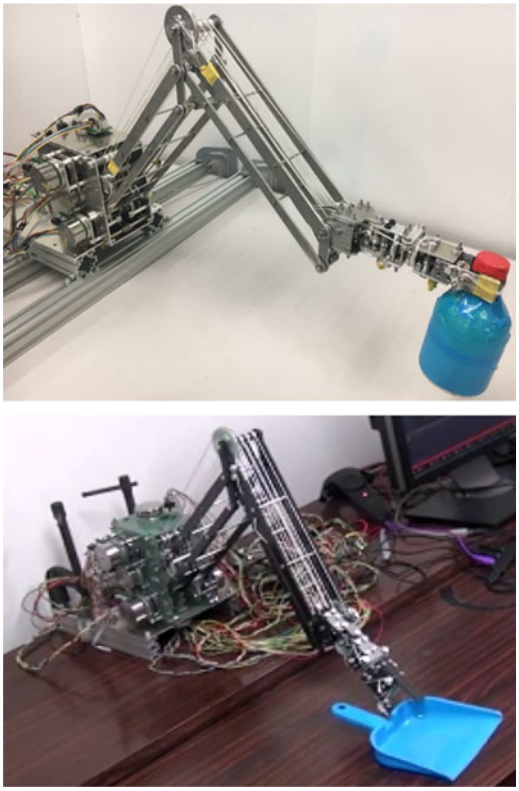

Fig. 10. Overview of developed robot (the upper robot is developed for gravity compensation experiments and the lower robot is developed for teleoperation experiments).

3.2. Specification

We developed two wire-driven robots with the above structure, as shown in Fig. 10. One robot is mainly composed of parts made of carbon-fiber-reinforced plastics (CFRP). The other robot is mainly composed of aluminium parts. The CFRP parts have lighter weight and higher stiffness than the aluminium parts. We used the robot with CFRP parts for the master–slave experiment because the lighter arm has better ability to carry out contact tasks, and the higher stiffness has better positioning performance. However, the CFRP parts have worse machinability, and we could not install the gravity and gripping force compensation mechanism on the robot. The aluminium parts have better machinability, which is good for prototyping. We then could install the proposed mechanism on the robot, and we used this robot for the gravity and gripping force compensation experiment.

Each robot had three 70-W brushless DC motors (EC 45 flat 70 W), manufactured by Maxon motor ag, for actuating the yaw base joint and the pitch joints of the shoulder and elbow. Each robot also had four 30-W brushless DC motors (EC 45 flat 30 W), manufactured by Maxon motor ag, for actuating the roll, pitch, and yaw joints of the wrist and the pitch joint of the gripper. Harmonic drives with a reduction ratio of 50:1 amplified the torque of these motors. We adopted cutting-edge Dyneema[29] as the material of the wires. Due to recent advances in materials[29] and heat treatment methods,[30] the mechanical properties of Dyneema have been dramatically improved. This greatly reduces concerns about elasticity, plasticity, and cutting of the wires.

The specifications of the robot with aluminium parts are shown in Table I. We here compare these specifications with those of a commercial industrial robot (LR Mate 200iD/4S) manufactured by Fanuc corporation. The specifications of LR Mate 200iD/4S are also shown in Table I. Therefore, the ratio of the payload weight to the total robot weight is much larger than that of the commercial robot. Note that the payload weight of the commercial robot becomes even smaller when a hand or gripper is attached to the robot because of the weight of the hand or the gripper. Although the information on the weight of the arm part of the commercial robot is unfortunately not disclosed, the weight of the hand-arm part of our robots seems to be about one-tenth of it. As a result, our robots significantly reduce the risk of damage to themselves and contacted objects when the robots perform contact tasks.

https://doi.org/10.1017/S0263574718001479 Published online by Cambridge University Press

Table I. Specifications.

	Developed robot (aluminium)	**Developed robot (CFRP)**	**LR Mate 200iD/4S**
Configuration	6-DoF arm with gripper	6-DoF arm with gripper	6-DoF arm
Size	Human arm size	Human arm size	Human arm size
Total weight (kg)	5.0	3.2	20
Weight of hand-arm part (kg)	1.0	0.6	10 (estimate)
Payload (kg)	0.6 (without compensation) 1.5 (with compensation)	0.6	4.0
Payload/weight ratio (–)	0.12 (without compensation) 0.3 (with compensation)	0.19	0.2

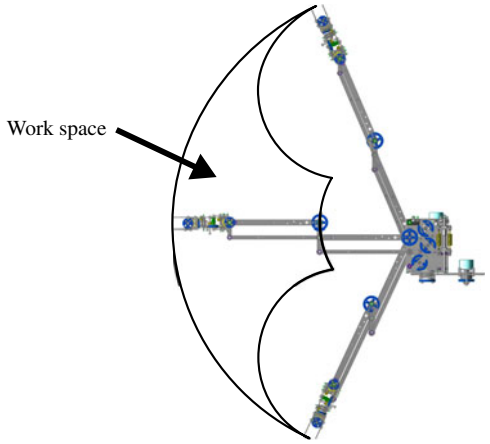

Fig. 11. Workspace of the developed robot.

The specifications of the robot with CFRP parts are shown in Table I. The total weight of this robot is 3.2 kg. The weight of the hand-arm part of this robot is 600 g. The payload weight without the compensation mechanism is 600 g.

3.3. Kinematics and dynamics of the proposed robot

We here derive kinematics and dynamics of the proposed robot. In this analysis, we use the relative joint angle $\boldsymbol{\theta} = (\theta_b, \theta_1, \theta_2, \theta_3, \theta_{wy}, \theta_{wr}, \theta_{gr})^T$ as shown in Fig. 6 instead of the absolute joint angle $q_i (i = 1, 2, 3)$ to derive dynamics with ordinary notation, where $\theta_b, \theta_1, \theta_2, \theta_3, \theta_{wy}, \theta_{wr}$, and $\theta_{gr} \in \mathbb{R}$ are the relative angles of the base joint, the shoulder joint, the elbow joint, the wrist pitch joint, the wrist yaw joint, the wrist roll joint, and the gripper joint, respectively. The three-dimensional tip position $\boldsymbol{x}(\boldsymbol{\theta}) = (x(\boldsymbol{\theta}), y(\boldsymbol{\theta}), z(\boldsymbol{\theta}))^T$ of the proposed robot is expressed by

$$x = (l_1 \cos\theta_1 + l_2 \cos(\theta_1 + \theta_2) + (l_3 + l_4 \cos\theta_{wy}) \cos(\theta_1 + \theta_2 + \theta_3)) \cos\theta_b \tag{17}$$

$$y = (l_1 \cos\theta_1 + l_2 \cos(\theta_1 + \theta_2) + (l_3 + l_4 \cos\theta_{wy}) \cos(\theta_1 + \theta_2 + \theta_3)) \sin\theta_b \tag{18}$$

$$z = l_1 \sin\theta_1 + l_2 \sin(\theta_1 + \theta_2) + (l_3 + l_4 \cos\theta_{wy}) \sin(\theta_1 + \theta_2 + \theta_3). \tag{19}$$

The kinematics is then almost the same as that of an articulated serial-link robot arm, which is one of the most common robot configurations.

The frontal workspace of the developed robot is shown in Fig. 11. Due to the parallel linkage, the join angle cannot exceed the region $\frac{\pi}{2} - 0.96 \leq q_i \leq \frac{\pi}{2} + 0.96$ $(i = 1, 2, 3)$ rad. The workspace of the developed robot is then narrower than typical serial-link robots. Nevertheless, the workspace covers an important range for carrying out various tasks.

The kinematic singularity of the developed robot is also the same as a typical serial-link robot, that is, the Jacobian matrix representing the relationship of infinitesimal displacement between the tip position and the joint angles loses rank when $\theta_1 = 0$, $\theta_2 = 0$, $\theta_3 = 0$, and $\theta_{wy} = 0$.

https://doi.org/10.1017/S0263574718001479 Published online by Cambridge University Press

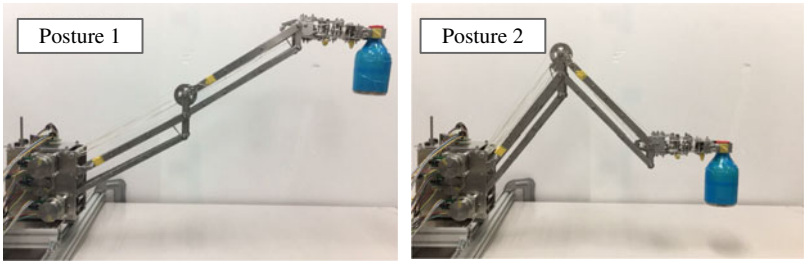

Fig. 12. Maintained postures in compensation experiment.

For more detailed kinematic analysis such as the condition number, manipulability, and so on, please see literatures of those of articulated robots.[27,28]

The dynamics of the proposed robot is the same as the dynamics of ordinary robots except that the wire tension T produces joint torques.

$$\boldsymbol{M}(\boldsymbol{\theta})\ddot{\boldsymbol{\theta}} + \boldsymbol{h}(\boldsymbol{\theta}, \dot{\boldsymbol{\theta}}) + \boldsymbol{g}(\boldsymbol{\theta}) = \boldsymbol{\tau} + \boldsymbol{J_w}(\boldsymbol{\theta})^T T, \tag{20}$$

where $\boldsymbol{M}(\boldsymbol{\theta}) \in \mathbb{R}^{7\times7}$ is the inertia matrix, $\boldsymbol{h}(\boldsymbol{\theta}, \dot{\boldsymbol{\theta}}) \in \mathbb{R}^7$ is the Coriolis and centrifugal vector, $\boldsymbol{g}(\boldsymbol{\theta}) \in \mathbb{R}^7$ is the vector of the gravity torque, $\boldsymbol{\tau} \in \mathbb{R}^7$ is the vector of the actuator torque, and $\boldsymbol{J_w}(\boldsymbol{\theta}) \in \mathbb{R}^7$ is the Jacobian matrix representing the relationship between joint velocity vector and velocity of the length of the wire path $\dot{\boldsymbol{\theta}} = \boldsymbol{J_w}(\boldsymbol{\theta})\dot{l}_w$.

4. Experiment

In order to confirm the effectiveness of the proposed mechanism, we conducted experiments using the developed robots described in the previous section.

4.1. Condition

We first describe the conditions of the gravity and gripping force compensation experiment. We used the sum of the squared current, which is required for the actuators to grip objects and maintain predetermined postures, to evaluate the reduction in power consumption due to the proposed compensation mechanism. The robot gripped and lifted several objects with different weights within the range that the robot could grip and lift. The robot maintained the two different postures as shown in Fig. 12. The wire tension was adjusted in order to compensate for the gravity torque in the Posture 2. When the robot switched postures while continuing to grip a certain object, we did not supply any power to the compensation actuator. This experiment was performed in two cases where the proposed mechanism was used and not used.

We conducted another master–slave experiment to verify the effectiveness of the proposed wire-driven mechanism in a contact task. A VR controller[31] was adopted as a master system. We obtained the 6-DoF information of the VR controller $\boldsymbol{x_c} = (x_c, y_c, z_c, q_{cp}, q_{cy}, q_{cr})^T$, where x_c, y_c, and $z_c \in \mathbb{R}$ are the three-dimensional position of the controller, and q_{cp}, q_{cy}, and $q_{cr} \in \mathbb{R}$ are the pitch, yaw, and roll angles of the controller, respectively. We used this 6-DoF information $\boldsymbol{x_c}$ as the desired tip position and attitude of the slave robot. Therefore, the vector of desired joint angle $\boldsymbol{\theta_d} = (\theta_{db}, \theta_{d1}, \theta_{d2}, \theta_{d3}, \theta_{dwy}, \theta_{dwr}, \theta_{dgr})^T$ was set so that $\boldsymbol{x}(\boldsymbol{\theta_d}) + \boldsymbol{x_b} = \boldsymbol{x_c}$, $\theta_{d1} + \theta_{d2} + \theta_{d3} = q_{cp}$, $\theta_{dwy} = q_{cy}$, and $\theta_{dwr} = q_{cr}$, where $\theta_{d*} \in \mathbb{R}$ is the desired value of θ_*, $\boldsymbol{x_b} = (x_b, y_b, z_b)^T$, and x_b, y_b, and $z_b \in \mathbb{R}$ are the bias constants of three-dimensional position. We also obtained analogue information on the degree of depression of the controller button $0 \le b \le 1 \in \mathbb{R}$ for opening and closing the robot gripper. The desired gripper angle was then set to $\theta_{dgr} = \theta_{grmin} + b(\theta_{grmax} - \theta_{grmin})$, where θ_{grmin} and $\theta_{max} \in \mathbb{R}$ are the minimum and maximum angles of the gripper joint, respectively. We adopted a PD controller to realize trajectory tracking.

$$\boldsymbol{\tau} = \boldsymbol{K_p}(\boldsymbol{\theta_d} - \boldsymbol{\theta}) - \boldsymbol{K_v}\dot{\boldsymbol{\theta}}, \tag{21}$$

where $\boldsymbol{K_p} = \mathrm{diag}(k_{pb}, k_{p1}, k_{p2}, k_{p3}, k_{pwy}, k_{pwr}, k_{pgr})$, $k_{pb}, k_{p1}, k_{p2}, k_{p3}, k_{pwy}, k_{pwr}$, and $k_{pgr} \in \mathbb{R}$ are position feedback gains, $\boldsymbol{K_v} = \mathrm{diag}(k_{vb}, k_{v1}, k_{v2}, k_{v3}, k_{vwy}, k_{vwr}, k_{vgr})$, and $k_{vb}, k_{v1}, k_{v2}, k_{v3}$, k_{vwy}, k_{vwr}, and $k_{vgr} \in \mathbb{R}$ are velocity feedback gains. A subject tried to pickup and handle a dustpan by using the master–slave system.

https://doi.org/10.1017/S0263574718001479 Published online by Cambridge University Press

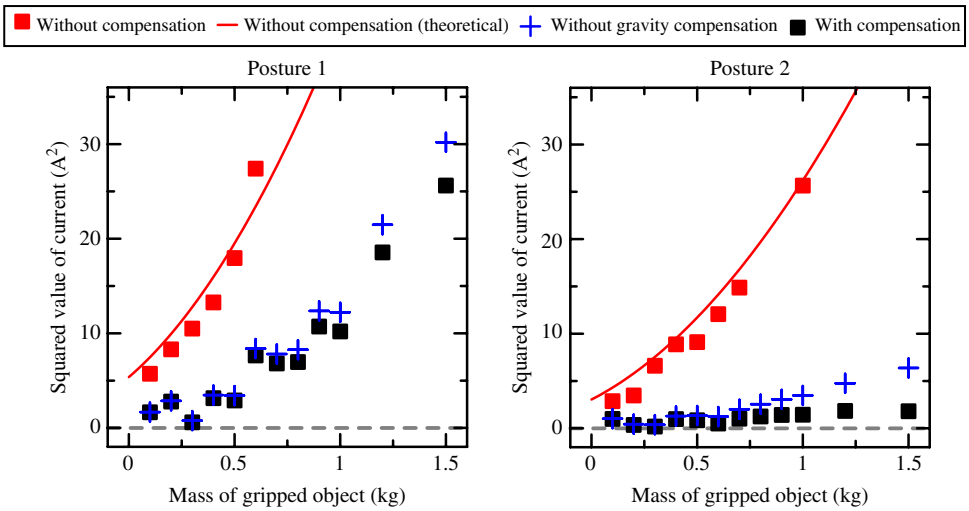

Fig. 13. Results of compensation experiment.

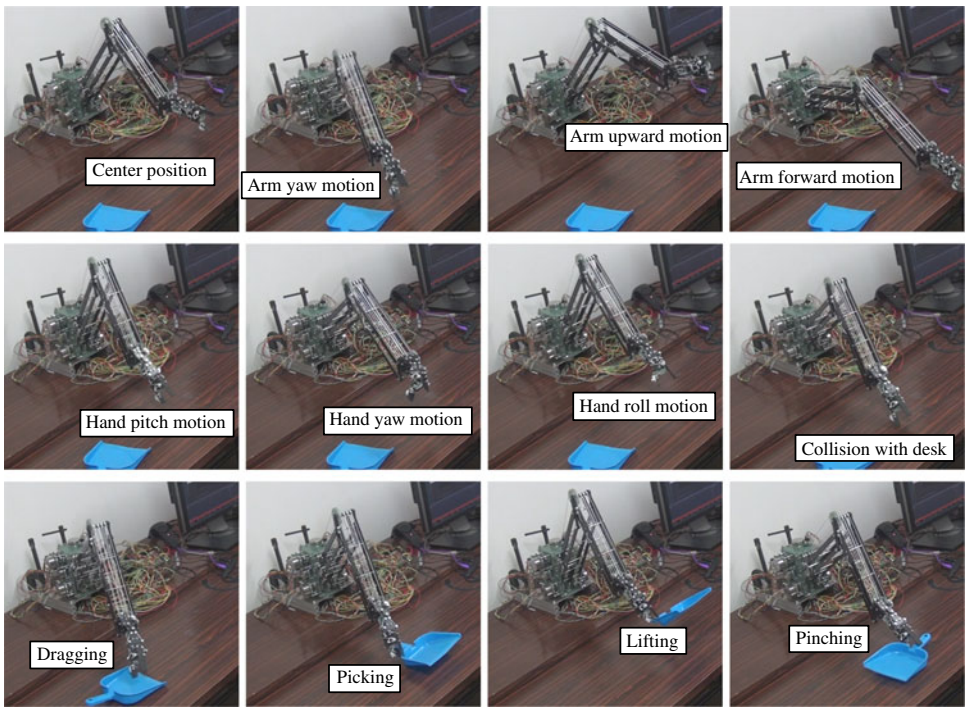

Fig. 14. Results of master–slave experiment.

4.2. Results

When the robot took the Posture 1, the measured joint angles were $\theta_1 = 2.7 \pm 0.10$ rad, $\theta_2 = 3.2 \pm 0.069$ rad, and $\theta_3 = 3.6 \pm 0.10$ rad. When the robot took the Posture 2, the measured joint angles were $\theta_1 = 2.4 \pm 0.083$ rad, $\theta_2 = 4.5 \pm 0.054$ rad, and $\theta_3 = 2.6 \pm 0.024$ rad. The current values when no compensation was applied almost agreed with the theoretical values as shown in Fig. 13. The proposed mechanism reduced the power consumption by 83% on average compared to the case without using the proposed mechanism, as shown in Fig. 13. The compensation rate was particularly high in the Posture 2 because we adjusted the wire tension so that the current values were the lowest in the posture. In the Posture 1, the current value increased quadratically as the mass of the gripped object increased. The reason seems that the actuator torque linearly increased due to changes in the wire tension and deflection of the links. Although the compensation rate was smaller in the

https://doi.org/10.1017/S0263574718001479 Published online by Cambridge University Press

Posture 1, the compensation rate still exceeded 77%. In other words, the proposed mechanism was able to compensate for most of the torque required to grip the object while supporting gravity.

In order to clarify the torque reduction effect of the gripping force compensation, we computed the current values necessary for the grasping and added them to the current values when the compensation was applied as shown in Fig. 13. The gripping force compensation did not significantly contribute to the reduction of the total current values. However, it is still an advantage that the proposed mechanism reduces the weight of the hand and the reduction ratio of the motor reducer of the gripper actuator.

In the master–slave experiment, this robot successfully generated 6-DoF motion as shown in Fig. 14. Even when the subject purposely slammed the robot hand into the desk, the robot and desk were not damaged and the subject could continue performing the task. The subject could drag and pickup the dustpan smoothly. Typical current industrial robots seem to be not easy to carry out these contact tasks. The subject were also able to pitch precisely the handle of the dustpan.

5. Conclusion

This paper has presented a simultaneous gravity and gripping force compensation mechanism for lightweight robots with low-reduction reducers. This mechanism is not placed on the hand-arm part of the robots and requires only one actuator for the compensation. Therefore, this mechanism greatly reduces the torque requirement of the joint actuators. The robots then can be lightweight and employ lower reduction ratio of motor reducers. These advantages are essential for future robots that will perform tasks in unstructured environments and collaborate with humans.

This paper also presented a novel structure for wire-driven robots to reduce the weight of the hand-arm part.

We developed two wire-driven robots that have the proposed compensation mechanism and novel structure to verify their effectiveness. The experimental results demonstrated that the proposed mechanism compensated for most of the torque required to grip and keep lifting objects. We also experimentally confirmed that the developed robot could carry out tasks without damaging robots and the environment even when the robots contacted the environment.

In the future, we will propose adaptive control methods that enable the proposed mechanism to grasp objects with unknown mass so that the proposed mechanism works in unstructured environments.

Supplementary Material

To view supplementary material for this article, please visit https://doi.org/S0263574718001479.

Acknowledgment

Funding from the NSK Foundation for the Advancement of Mechatronics is gratefully acknowledged.

References

1. A. Albu-Schaffer, O. Eiberger, M. Grebenstein, S. Haddadin, C. Ott, T. Wimbock, S. Wolf and G. Hirzinger, "Soft robotics," *IEEE Rob. Autom. Mag.* **15**(3), 20–30 (2008).
2. N. Salomonski, M. Shoham and G. Grossman, "Light robot arm based on inflatable structure," *CIRP Ann. Manuf. Technol.* **44**(1), 87–90 (1995).
3. S. Sanan, J. B. Moidel and C. G. Atkeson, "Robots with Inflatable Links," *IEEE/RSJ International Conference on Intelligent Robots and Systems* (2009), pp. 4331–4336.
4. D. G. Caldwell, G. A. Medrano-Cerda and M. J. Goodwin, "Braided Pneumatic Actuator Control of a Multi-jointed Manipulator," *International Conference on Systems, Man and Cybernetics*, vol. 1 (1993) pp. 423–428.
5. K. Hosoda, T. Takuma, A. Nakamoto and S. Hayashi, "Biped robot design powered by antagonistic pneumatic actuators for multi-modal locomotion," *Rob. Auton. Syst.* **56**(1), 46–53 (2008).
6. G. A. Pratt and M. M. Williamson, "Series Elastic Actuators," *IEEE/RSJ International Conference on Intelligent Robots and Systems*, vol. 1 (1995) pp. 399–406.
7. Rethink Robotics Baxter website: http://www.rethinkrobotics.com/baxter/.
8. H. Asada and K. Youcef-Toumi, "Analysis and Design of Semi-Direct-Drive Robot Arms," *American Control Conference* (1983).
9. H. Asada and K. Youcef-Toumi, "Analysis and design of a direct-drive arm with a five-bar-link parallel drive mechanism," *J. Dyn. Syst. Meas. Control* **106**, 225–230 (1984).

10. D. Ogane, K. Hyodo and H. Kobayashi, "Mechanism and control of a 7 D.O.F. tendon-driven robotic arm with NST," *J. Rob. Soc. Jpn.* **14**(8), 1152–1159 (1996). (In Japanese).
11. B. Rooks, "The harmonious robot," *Ind. Rob. Int. J. Rob. Res. Appl.* **33**(2), 125–130 (2006).
12. Barrett Technology, LLC. http://www.barrett.com/products-arm.htm.
13. 3D Systems, Inc. http://www.geomagic.com/en/products/phantom-premium/overview.
14. M. Quigley, A. Asbeck and A. Ng, "A low-cost compliant 7-DOF robotic manipulator," *IEEE International Conference on Robotics and Automation* (2011) pp. 6051–6058.
15. Y. Tsumaki, S. Shimanuki, F. Ono and H. Han, "Ultra-Lightweight Forearm with a Parallel-Wire Mechanism," *IEEE/ASME International Conference on Advanced Intelligent Mechatronics* (2014) pp. 1419–1423.
16. Y. J. Kim, "Design of Low Inertia Manipulator with High Stiness and Strength Using Tension Amplifying Mechanisms," *IEEE/RSJ International Conference on Intelligent Robots and Systems* (2015) pp. 5850–5856.
17. N. Ulrich and V. Kumar, "Passive Mechanical Gravity Compensation For Robot Manipulators," *IEEE International Conference on Robotics and Automation* (1991) pp. 1536–1541.
18. S. Hirose, T. Ishii and A. Haishi, "Float Arm V: Hyper-Redundant Manipulator With Wire-Driven Weght-Compensation Mechanism," *IEEE International Conference on Robotics and Automation* (2003) pp. 368–373.
19. T. Morita, F. Kuribara, Y. Shiozawa and S. Sugano, "A Novel Mechanism Design for Gravity Compensation in Three Dimensional Space," *IEEE/ASME International Conference on Advanced Intelligent Mechatronics* (2003) pp. 163–168.
20. A. Fattah and S. K. Agrawal, "Gravity-Balancing of Classes of Industrial Robots," *IEEE International Conference on Robotics and Automation* (2006) pp. 2872–2877.
21. T. Naoyuki, I. Takashi, M. Hideyuki and F. Hideo, "Design and prototype of Variable Gravity Compensation Mechanism (VGCM)," *J. Rob. Mechatron.* **23**(2), 249–257 (2011).
22. D. G. Lee and T. W. Seo, "Lightweight Multi-DOF Manipulator with Wire-Driven Gravity Compensation Mechanism," *IEEE/ASME Trans. Mechatron.* **22**(3), 1308–1314 (2017).
23. H. Nakamoto and N. Matsuhira, "Development of an Arm for Collaborative Robot Equipped with Gravity Compensation Mechanism According to Payload," *IEEE International Conference on Advanced Intelligent Mechatronics* (2017).
24. S. C. Jacobsen, E. K. Iversen, D. F. Knutti, R. T. Johnson and K. B. Biggers, "Design of the Utah/Mit Dexterous Hand," *IEEE International Conference on Robotics and Automation* (1996) pp. 1520–1532.
25. Y. Ogahara, Y. Kawato, K. Takemura and T. Maeno, "A Wire-Driven Miniature Five Fingered Robot Hand Using Elastic Elements as Joints," *IEEE/RSJ International Conference on Intelligent Robots and Systems* (2003) pp. 2672–2677.
26. Y. Kurita, Y. Onoo, A. Ikedao and T. Ogasawara, "NAIST Hand 2: Human-Sized Anthropomorphic Robot Hand with Detachable Mechanism at the Wrist," *IEEE/RSJ International Conference on Intelligent Robots and Systems* (2009) pp. 2271–2276.
27. J. K. Salisbury and J. J. Craig, "Articulated hands: Force control and kinematic issues," *Int. J. Rob. Res.* **1**(1), 4–17 (1982).
28. T. Yoshikawa, "Manipulability of robotic mechanisms," *Int. J. Rob. Res.* **4**(2), 3–9 (1985).
29. Dyneema website: https://www.dsm.com/products/dyneema/en_GB/home.html.
30. TEUFELBERGER Fiber Rope Corporation website: https://www.neropes.com/products/performance/products/detail/Product/hsr-75/.
31. VR system VIVE website: https://www.vive.com/jp/.

https://doi.org/10.1017/S0263574718001479 Published online by Cambridge University Press